

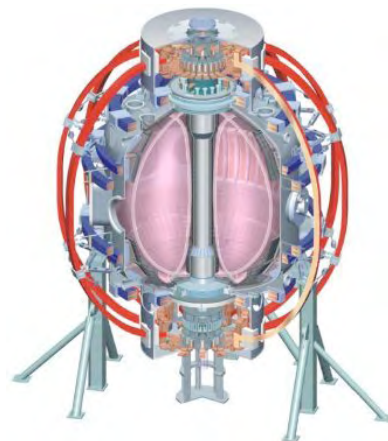
# The Motional Stark Effect Diagnostic on NSTX

**Fred M. Levinton, Nova Photonics**

Howard Yuh, Nova Photonics,  
and the NSTX Research Team

College W&M  
Colorado Sch Mines  
Columbia U  
Comp-X  
General Atomics  
INEL  
Johns Hopkins U  
LANL  
LLNL  
Lodestar  
MIT  
Nova Photonics  
New York U  
Old Dominion U  
ORNL  
PPPL  
PSI  
Princeton U  
SNL  
Think Tank, Inc.  
UC Davis  
UC Irvine  
UCLA  
UCSD  
U Colorado  
U Maryland  
U Rochester  
U Washington  
U Wisconsin

**50 th Annual Meeting of the Division of Plasma  
November 17-21, 2008  
Dallas, TX**



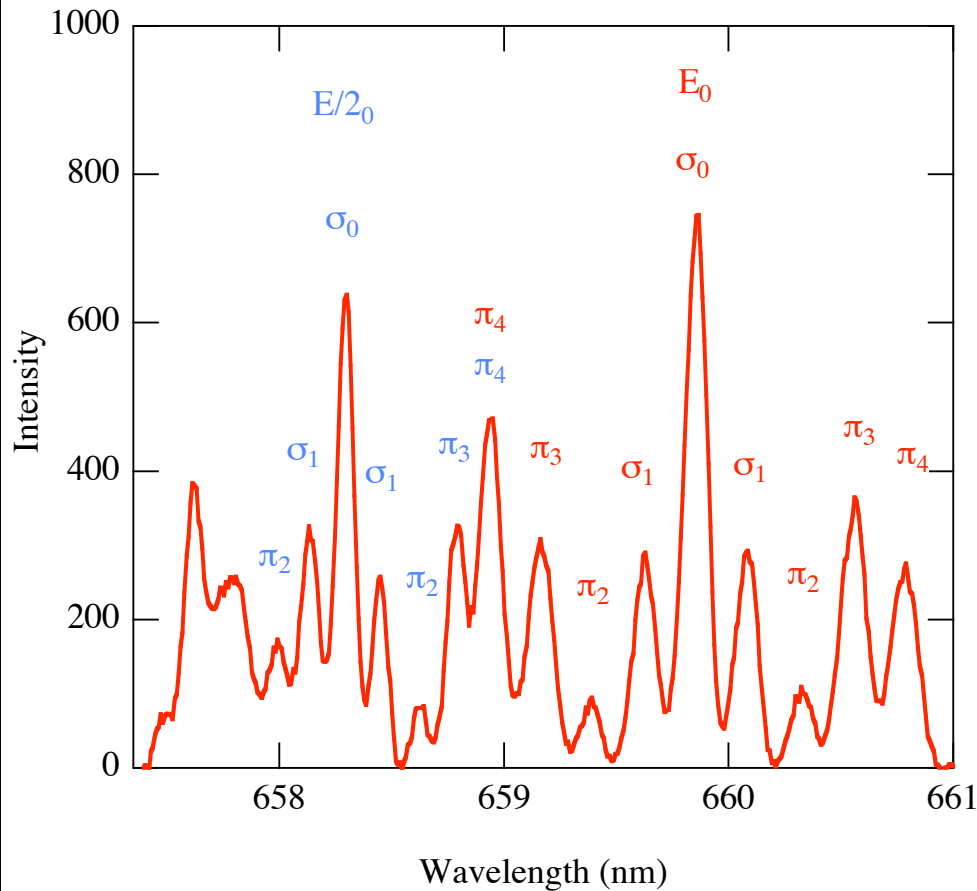
Culham Sci Ctr  
U St. Andrews  
York U  
Chubu U  
Fukui U  
Hiroshima U  
Hyogo U  
Kyoto U  
Kyushu U  
Kyushu Tokai U  
NIFS  
Niigata U  
U Tokyo  
JAEA  
Hebrew U  
Ioffe Inst  
RRC Kurchatov  
Inst  
TRINITY  
KBSI  
KAIST  
POSTECH  
ASIPP  
ENEA, Frascati  
CEA, Cadarache  
IPP, Jülich  
IPP, Garching  
ASCR, Czech Rep  
U Quebec

# ABSTRACT

This work describes the implementation and recent results from the MSE-CIF diagnostic on NSTX. Due to the low magnetic field on NSTX the MSE diagnostic requires a new approach for the viewing optics and spectral filter. This has been accomplished with a novel optical design that reduces the geometric Doppler broadening, and a high throughput, high resolution spectral filter to optimize signal-to-noise. This MSE diagnostic presently has 16 sightlines operating, providing measurements of the magnetic field line pitch from the plasma center to near the outboard edge of the plasma. Due to the low magnetic field ( $\sim 0.35$  Tesla) the Stark splitting is small, thus several changes from typical MSE diagnostics were incorporated into the system. The optical system is configured using an aperture to reduce the geometric Doppler broadening from the heating beam and increase the polarization fraction. Another innovation was development of a birefringent interference filter with high throughput and high resolution. With the narrow bandwidth filter the polarization fraction is  $\sim 30\text{-}40\%$  and combined with the large throughput results in a time resolution of  $\sim 5$  ms.

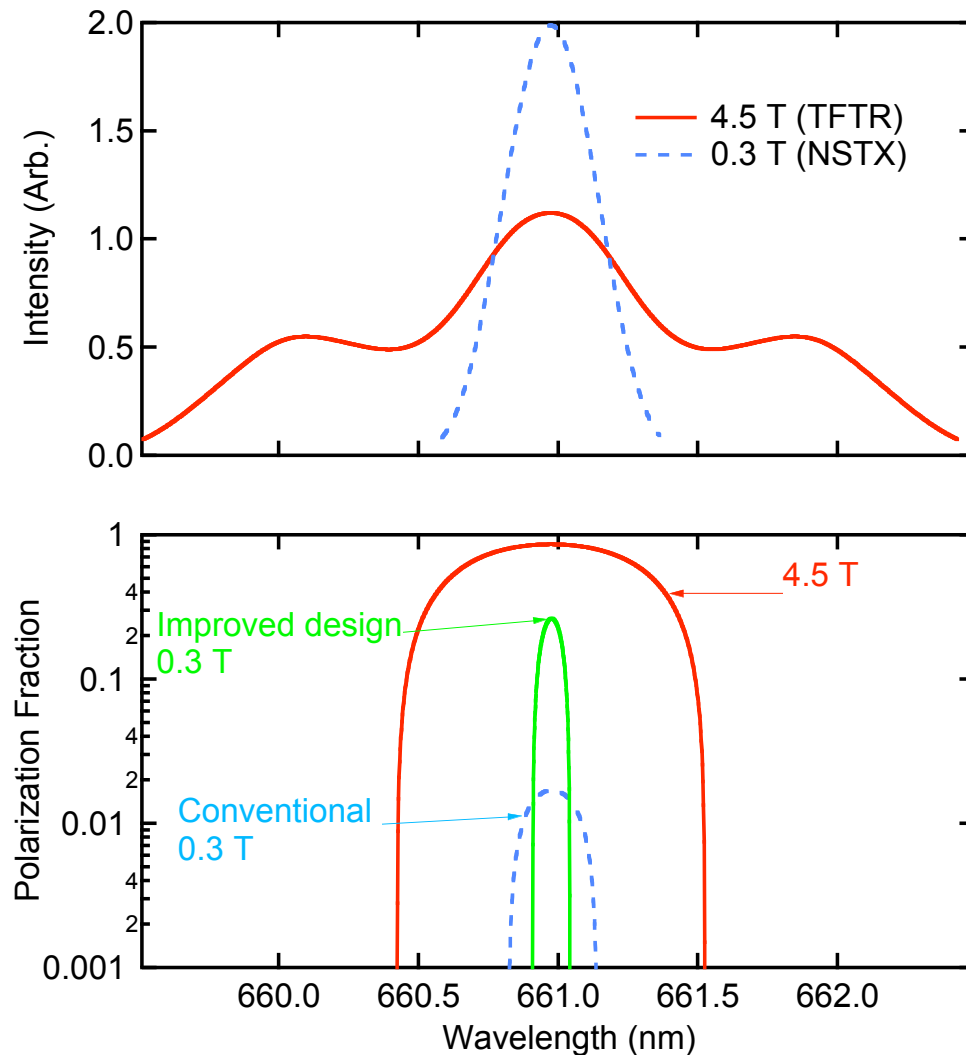
This work supported by U.S. DOE contracts DE-FG02-99ER54520 and DE-AC02-76CH03073.

# MSE Spectra at High Magnetic Field



- $\mathbf{E}=\mathbf{v} \times \mathbf{B}$  electric field  $\sim 200$  kV/cm at 4.5 T in figure.
- $\Delta m=0(\pm 1)$ ,  $\pi(\sigma)$ , are polarized parallel(perpendicular) to the electric field.
- Spectral width is determined by geometric broadening and beam divergence.
- Spectral overlap between  $\pi$  and  $\sigma$  lines reduces polarization fraction and signal-to-noise.

# Polarization Modeling

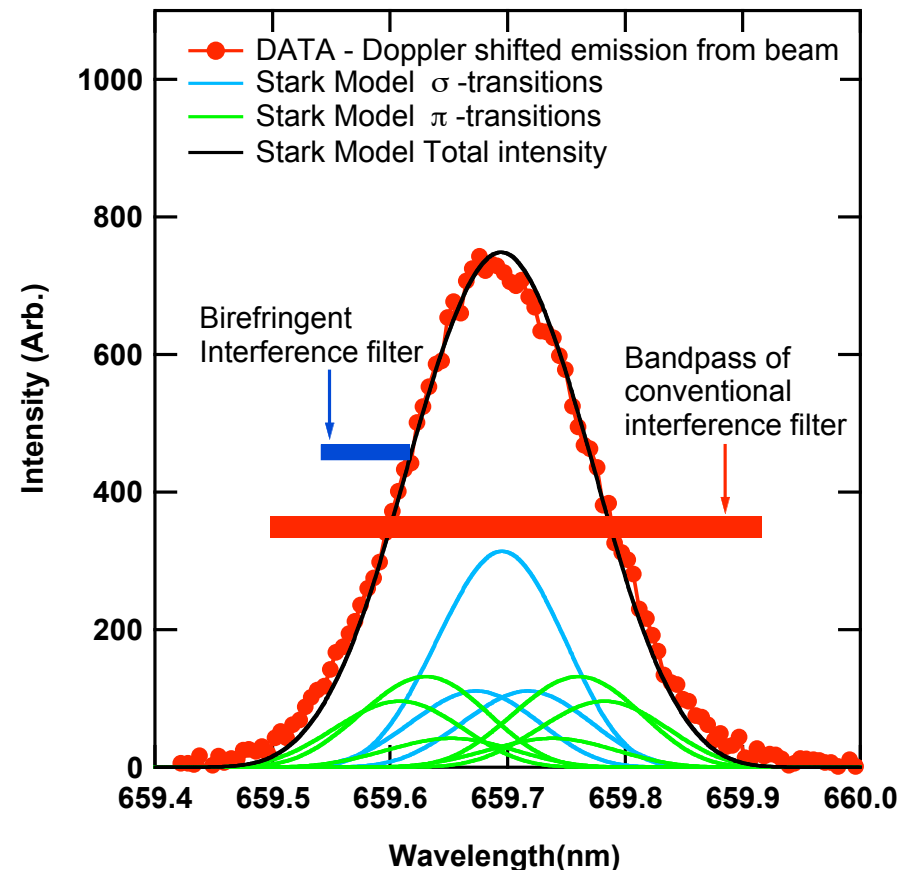


Numerical convolution of MSE spectra including filter, beam, optics broadening.

Using conventional approach, overlap of spectral lines leads to a low ( $\sim 1\%$ ) polarization fraction. With improvements in the optics design and filter bandwidth, the polarization fraction can be raised to 30-40%.

# Successful MSE-CIF Polarimetry Measurements at Low Magnetic Field

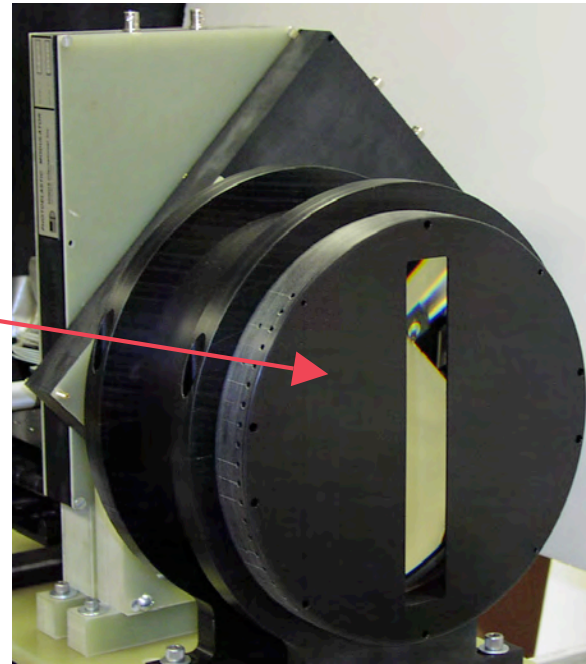
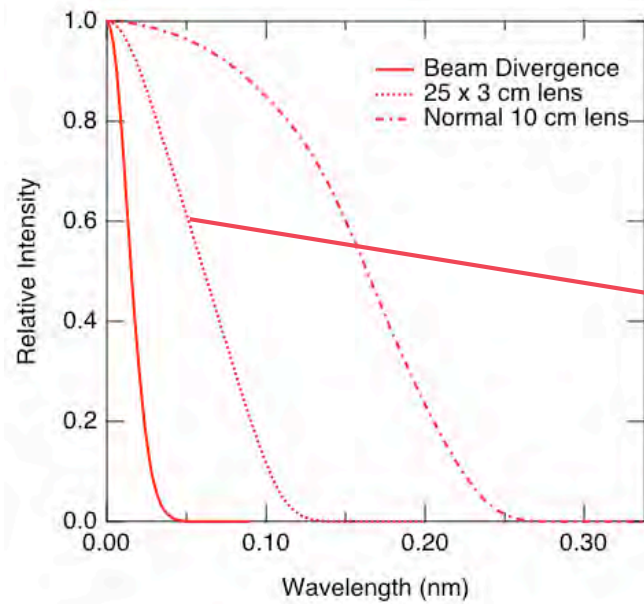
- At low magnetic field, overlap of Stark multiplet results in low polarization fraction ( $\sim 2\%$ ) with conventional filter.
- Novel birefringent filter with narrow bandpass can isolate a portion of the spectrum resulting in a much better polarization fraction ( $\sim 40\%$ ).
- Allows MSE-CIF measurements at low magnetic field with good time resolution (5 ms).



## MSE-CIF at Low Magnetic Field

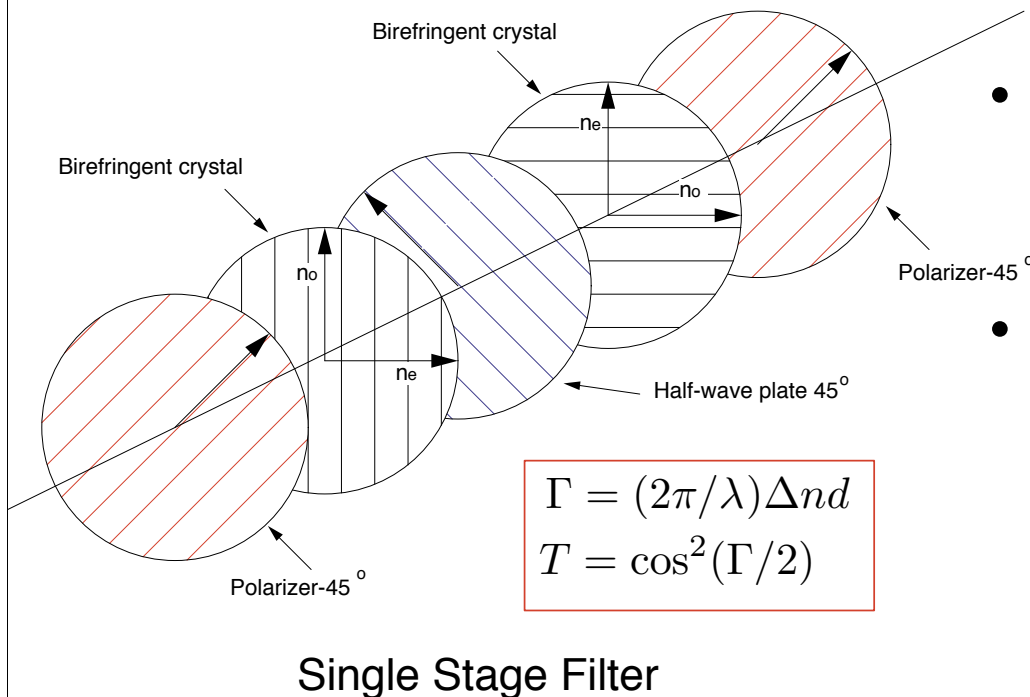
- Innovations to improve the polarization fraction.
  - ➔ Optimize optics to minimize geometric Doppler broadening.
  - ➔ Development of high resolution, high throughput filter to extend measurements to 0.3 T. Wide field Lyot birefringent filter meets these requirements.

# Novel Optics Design



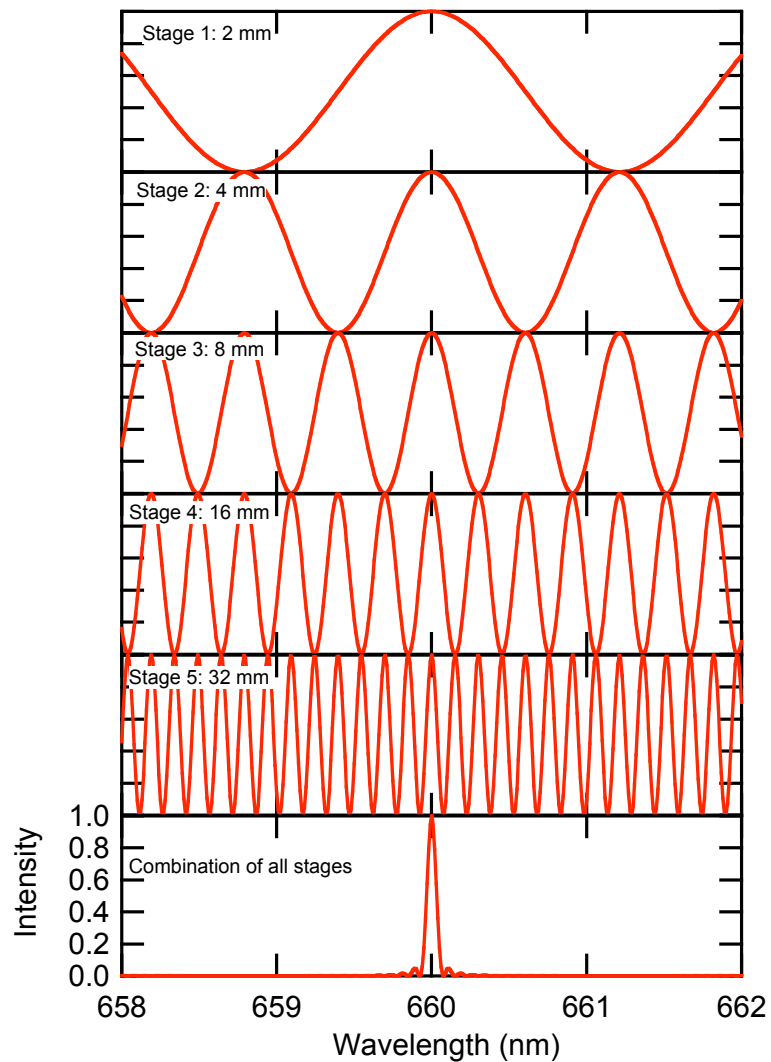
- Novel optics design reduces geometric Doppler broadening.

# Wide Field Birefringent Interference Filter(BIF)



- Single stage of wide field birefringent interference filter (Lyot type).
- Flexible in combining multiple stages to form desired spectral filter.
- Increased luminosity by a factor of 20-1000 relative to other instruments (grating spectrometer, Fabry-Perot, interference filter).

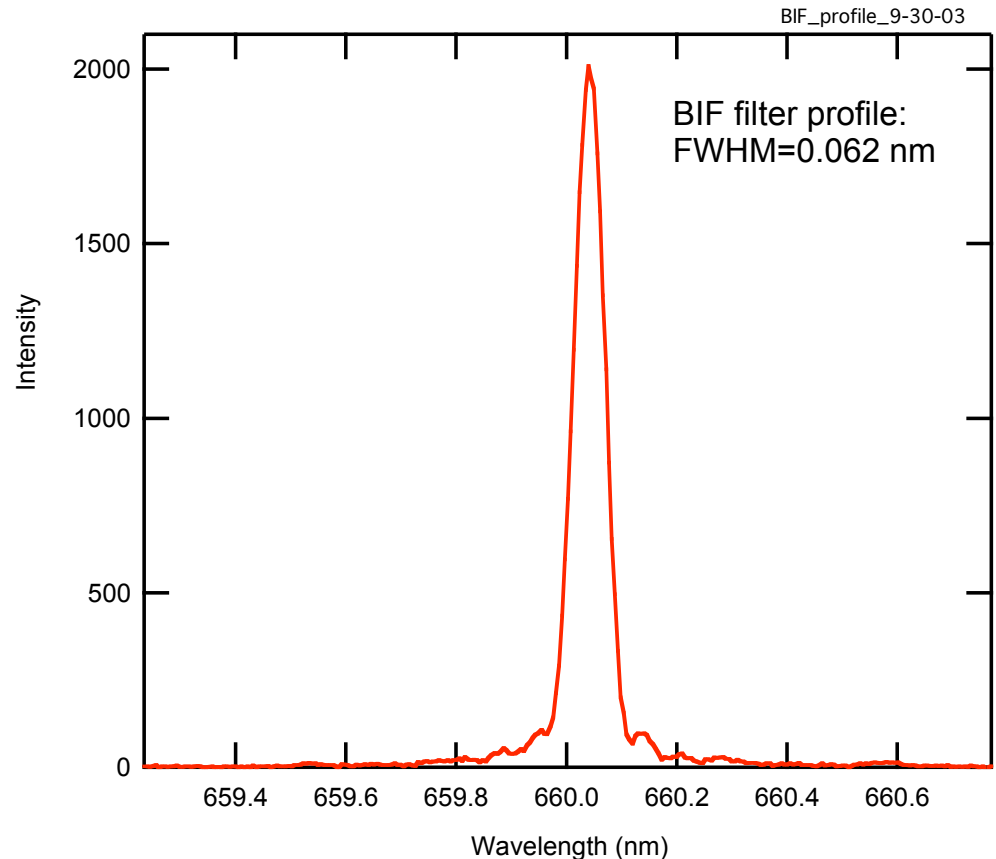
# Combination of BIF Stages



- Model of five BIF stages combined to produce wide field, narrow band spectral filter.

## Birefringent Filter for NSTX

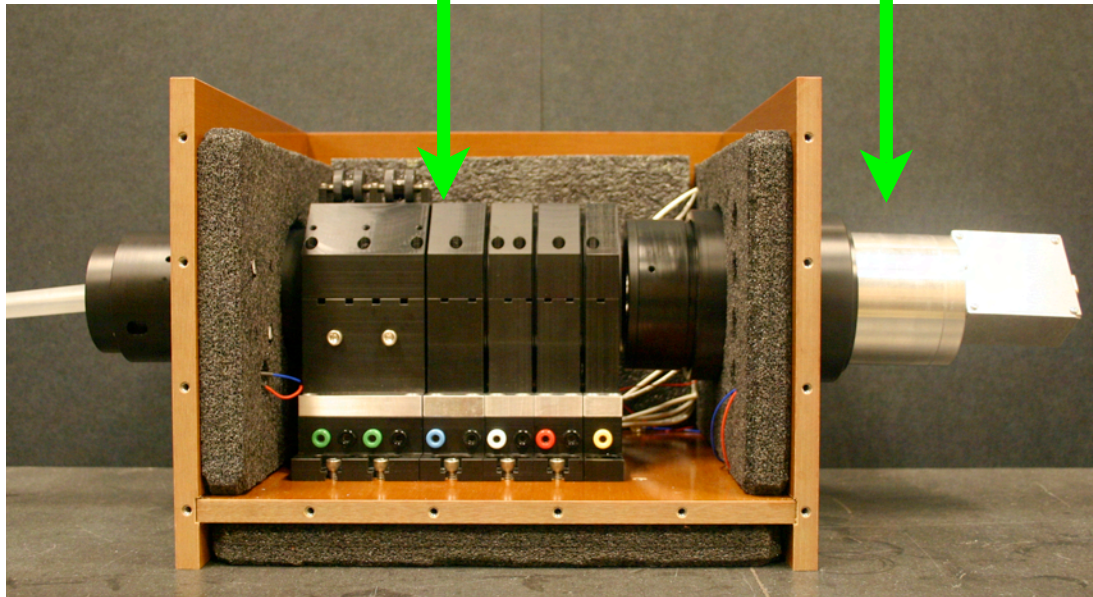
- Novel high throughput, narrow passband filter makes measurements with MSE at low field possible.
- Overall design has resulted in a polarization fraction greater than 40% .
- Achieved good time resolution( $\sim 5$  ms).



## Novel Lyot Birefringent Filter

5-stage Filter

Detector



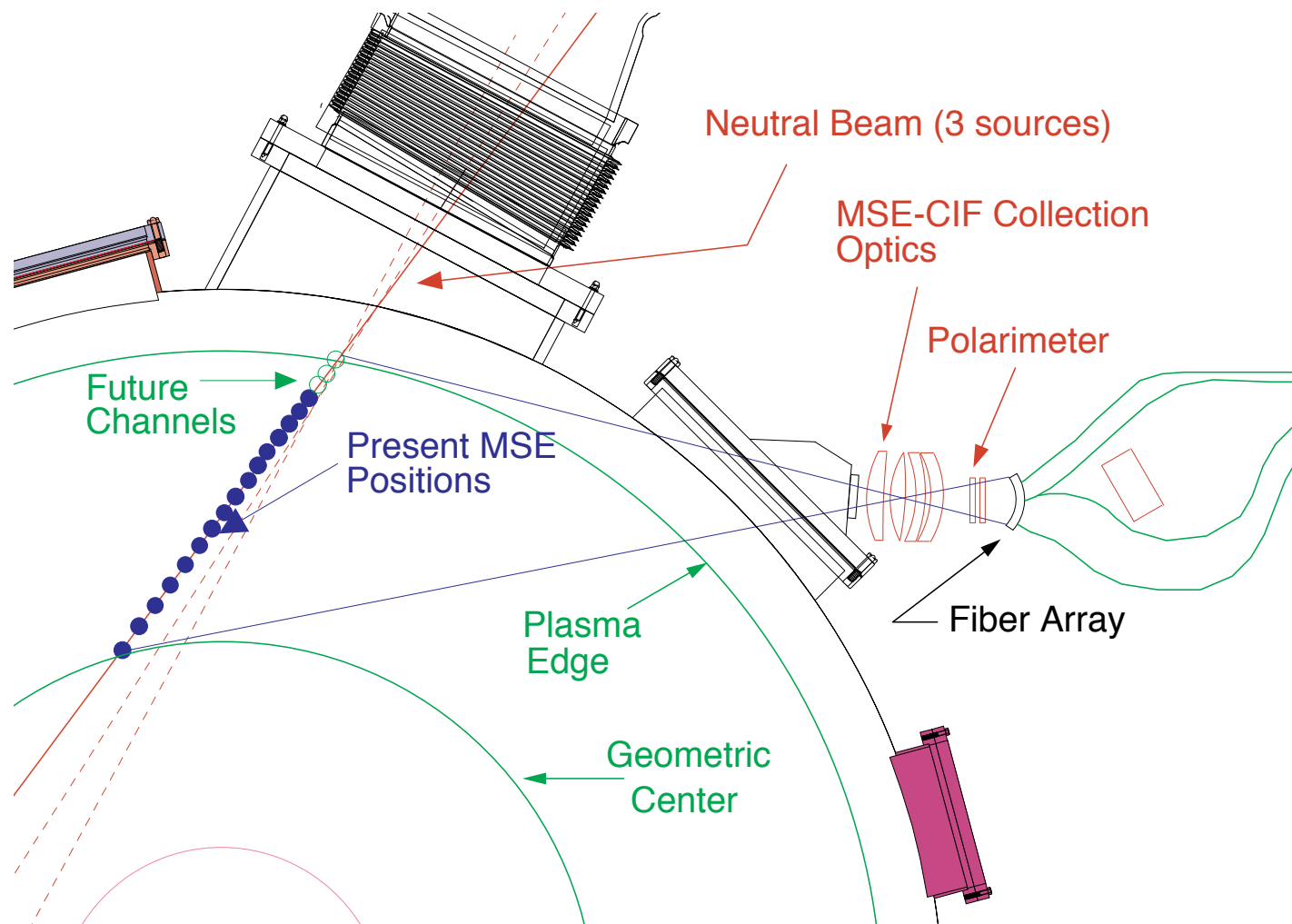
- High throughput, narrow passband filter makes measurements with MSE at low field possible with time resolution of 5-10 ms.
- Modular filter has a 75 mm clear aperture, wide field of view, narrow bandwidth, and is tunable.

# BIF has Large Throughput Advantage Over Other Instruments

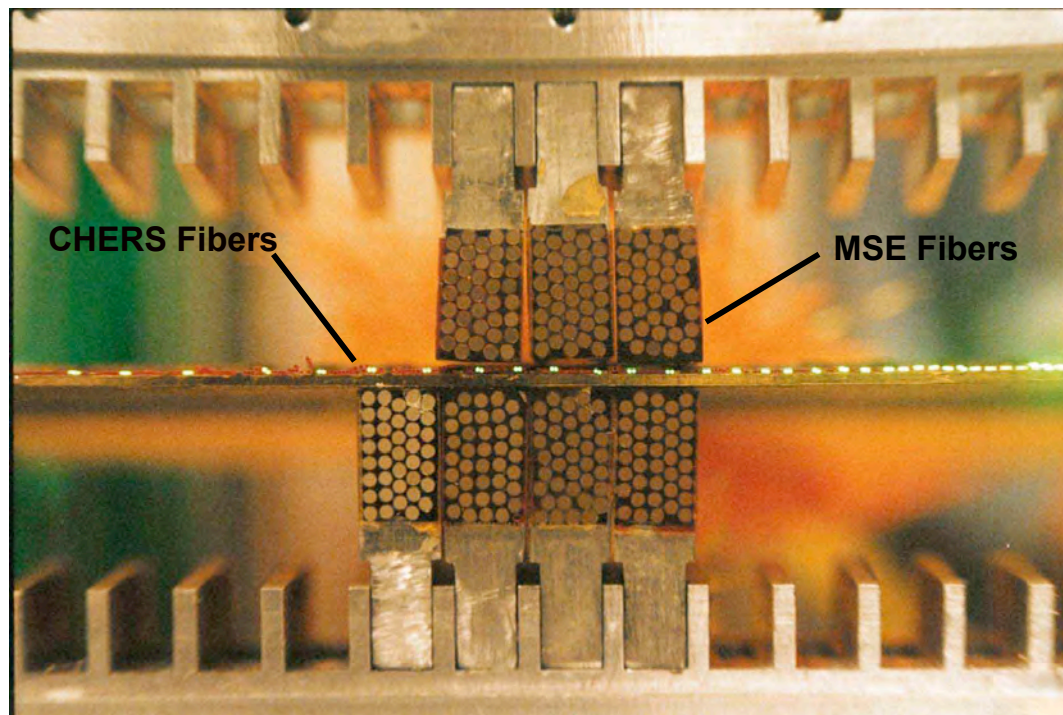
Instrument	Input aperture A(mm <sup>2</sup> )	resolution (nm)	f/#	Etendue U(mm <sup>2</sup> -sr)	Transmission <i>t</i>	Luminosity	Throughput Relative to BIF(NSTX)
BIF(NSTX)	59.7	0.062	1.2	32.6	10%	3.3	1
BIF (achievable)	4560.4	0.17	1.58	1434.8	30%	430.4	130.4
Fabry-Perot	1	0.062	1.2	0.5	25%	0.13	1/25
Grating(reflection)	0.04	0.1	5	10 <sup>-3</sup>	80%	8x10 <sup>-4</sup>	1/(4x10 <sup>3</sup> )
Grating(transmission)	0.04	0.1	1.8	10 <sup>-2</sup>	80%	8x10 <sup>-5</sup>	1/400

$$U = \pi A(NA)^2 = \pi A/4f^2$$

# MSE-CIF Layout on NSTX

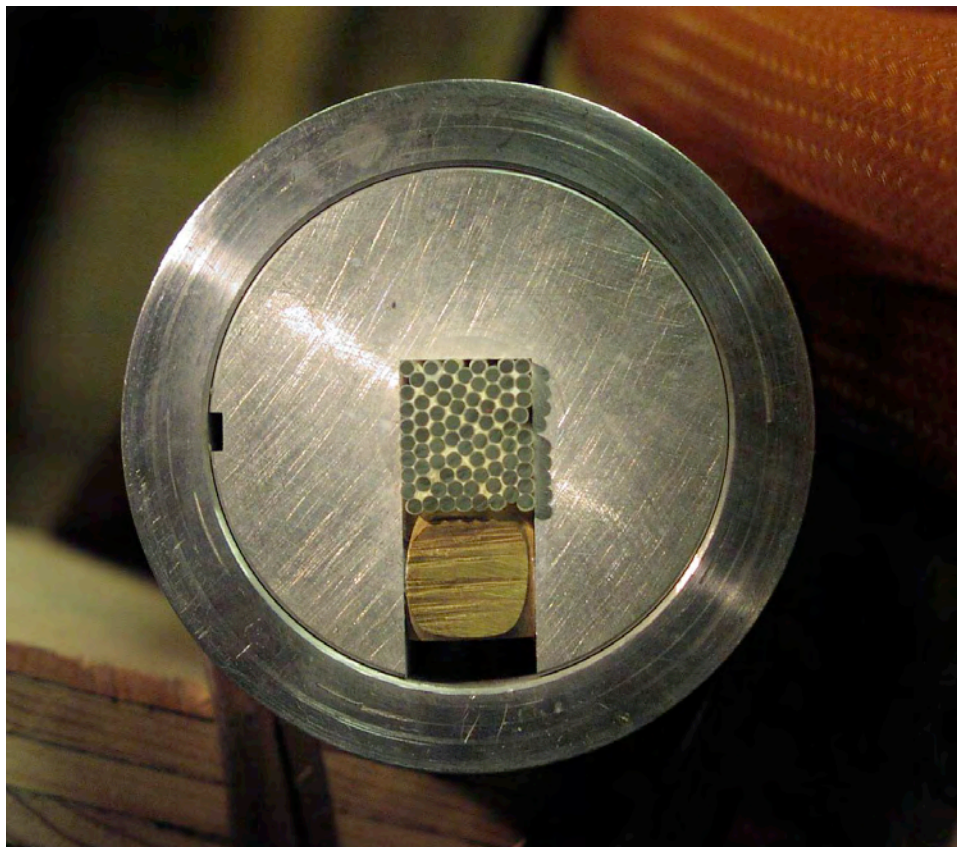


## MSE & CHERS Fiber Optic Holder



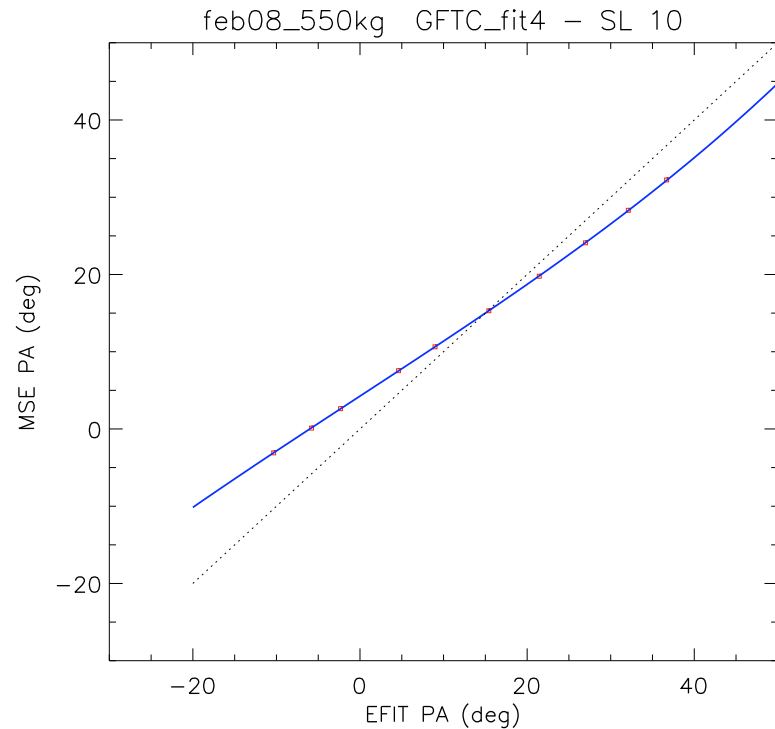
- View of fiber holder with a few fiber ferrules installed.
- CHERS fibers are the small fibers in the midplane.

## Output Fiber Bundle



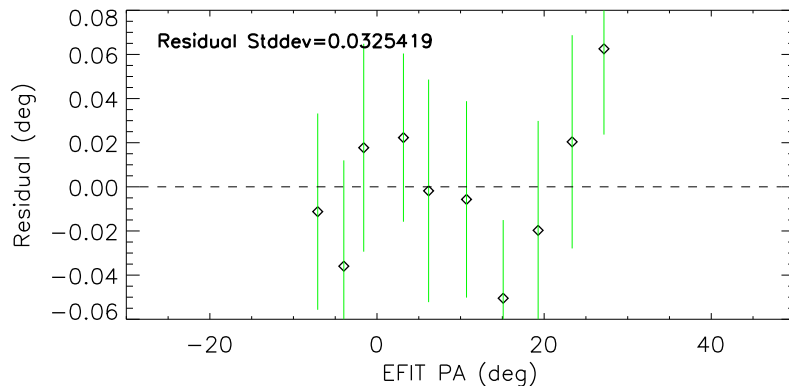
- Input fiber bundle to BIF.
- Each fiber optic bundle contains 76 x 1 mm fibers.

# Beam into Gas used for Calibration

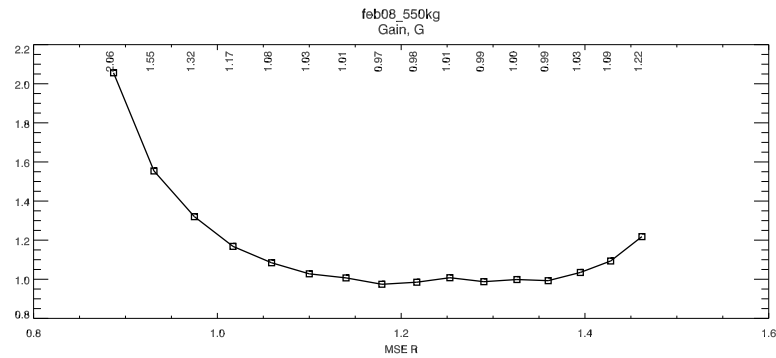
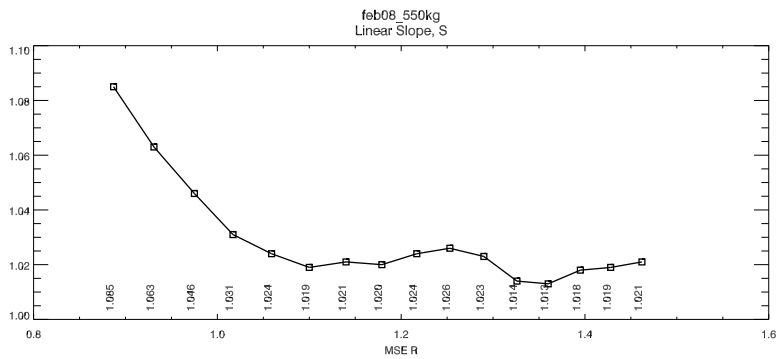
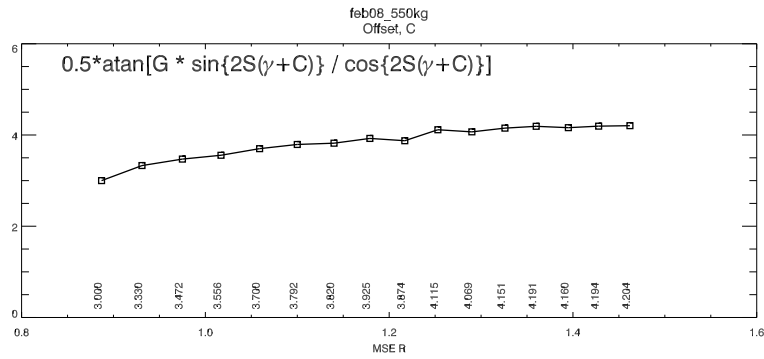


- Beam into gas used for calibration.
- Typical fit and residuals shown for one sightline.
- Fitting function:

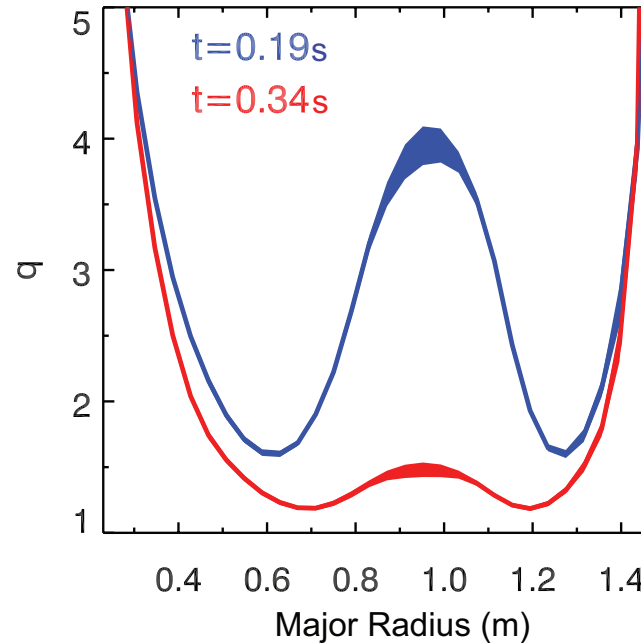
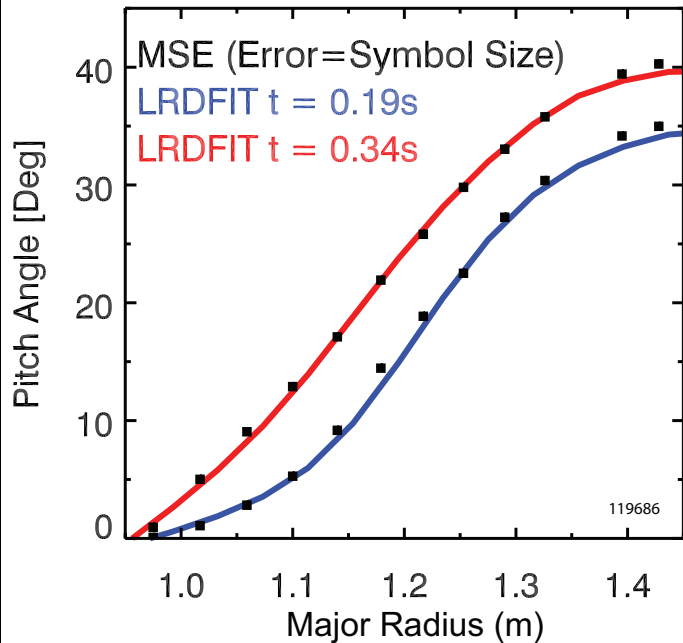
$$\gamma_{MSE} = 0.5 * \tan^{-1} \left[ \frac{G * \sin(2S(\gamma + C))}{\cos(2S(\gamma + C))} \right]$$



# Calibration-Fitted Parameters

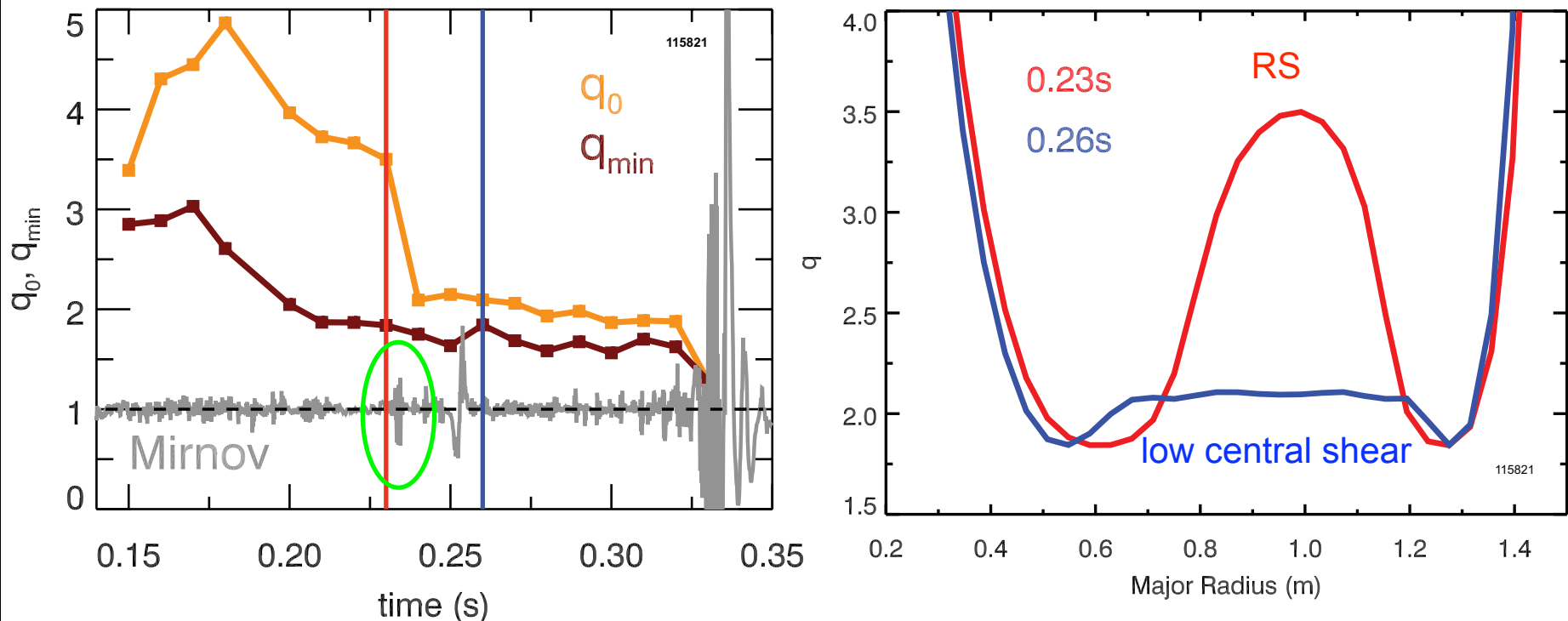


# Equilibrium Reconstruction with MSE



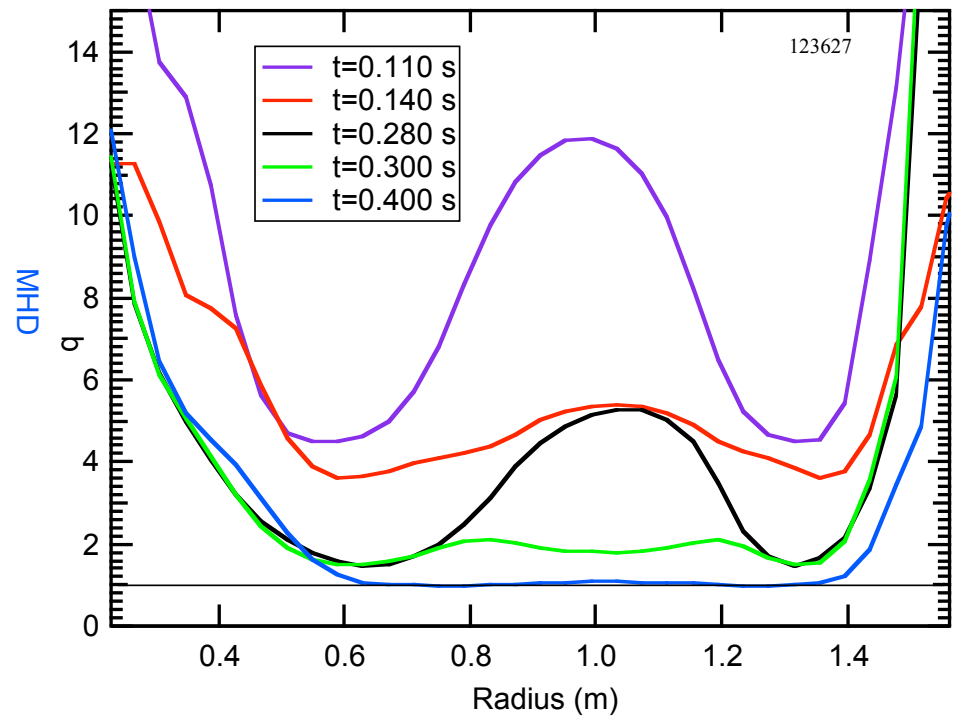
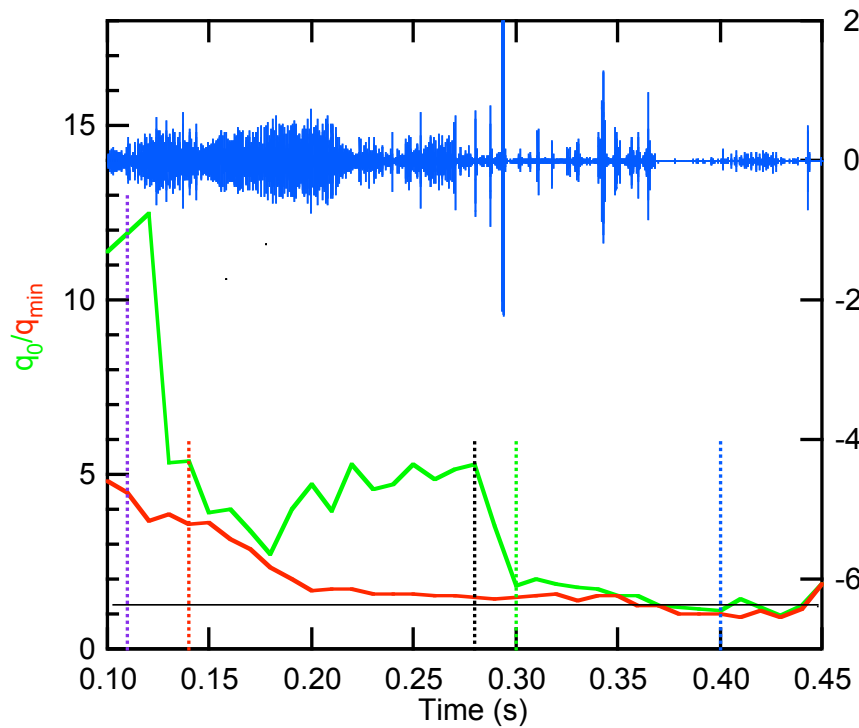
- Use LRDFIT, a free boundary equilibrium reconstruction code (J. Menard). Includes  $T_e$  iso-surfaces and toroidal rotation.
- Fits with MSE data have low residuals of  $\sim 0.3^\circ$  in core, but higher at edge.
- $E_r$  correction from  $V_\phi$  and  $\nabla p$  included, but not from  $V_\theta$ .
- Variability of LRDFIT reconstruction shown in bands.

## Low Shear q-profile After MHD Reconnection

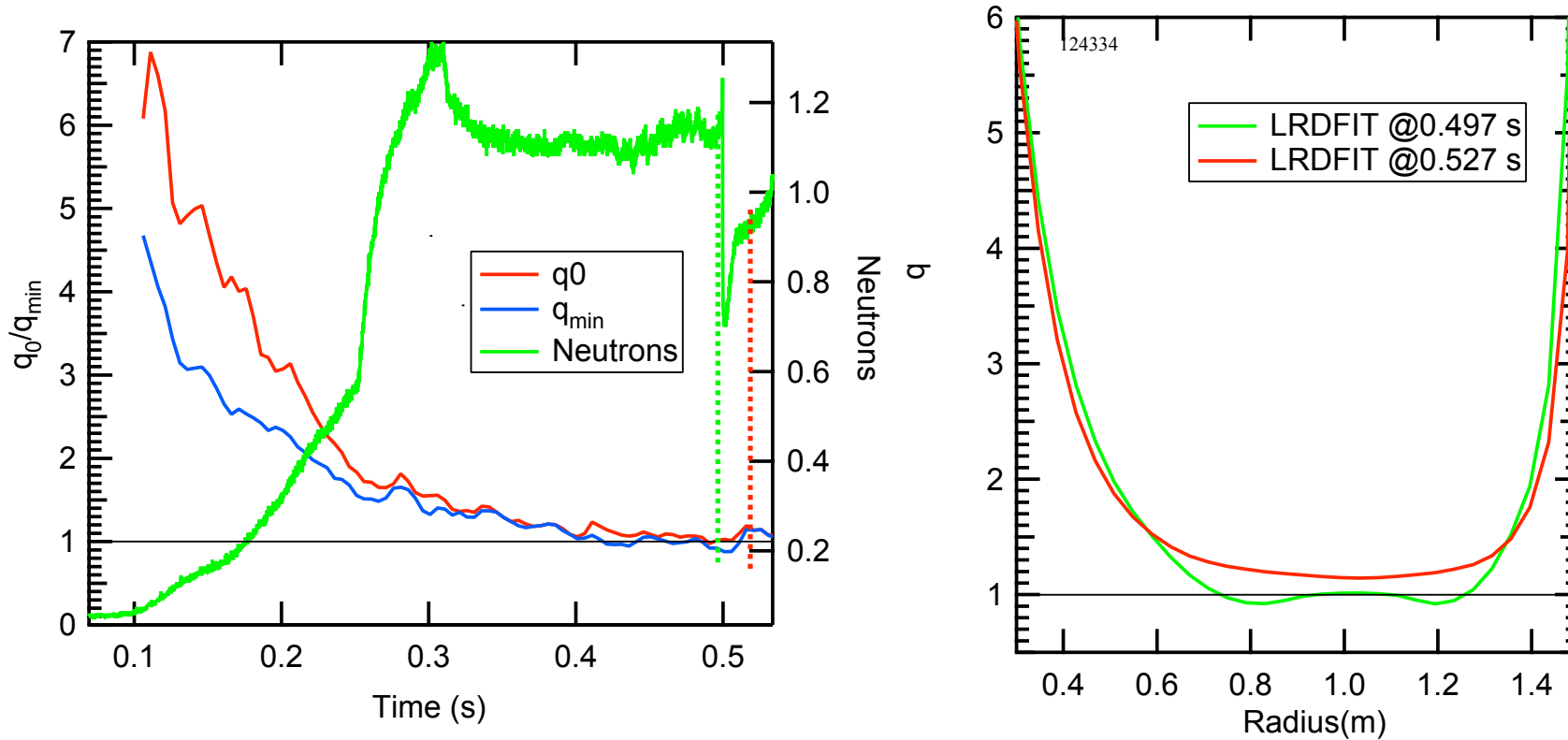


- MHD ( $m/n=2/1$ ) event precipitates a large change in  $q(0)$ .
- Rapid change occurs shortly after  $q_{\min}$  drops below 2.
- $q$ -profile flattened at  $q=2$ .

# MHD Causes Current Redistribution



# Sawtooth like Event with Reversed Shear Can Raise $q(0)$ above 1.



## Fluctuations Observed in MSE Measurements

$$\begin{aligned} I = & I_0(1 + \alpha \sin(\omega t)) \left(1 + \frac{1}{\sqrt{2}} J_0(\pi) \{ \cos[2(\gamma + \tilde{\gamma} \sin(\omega t))] + \sin[2(\gamma + \tilde{\gamma} \sin(\omega t))] \} \right) \\ & + \sqrt{2} J_2(\pi) \{ \cos[2(\gamma + \tilde{\gamma} \sin(\omega t))] \cos(2\Omega_1 t) + \sin[2(\gamma + \tilde{\gamma} \sin(\omega t))] \cos(2\Omega_2 t) \} \\ & + 2\sqrt{2} J_1^2(\pi) \sin(\Omega_1 t) \sin(\Omega_2 t) \cos[2(\gamma + \tilde{\gamma} \sin(\omega t))] + \dots \end{aligned}$$

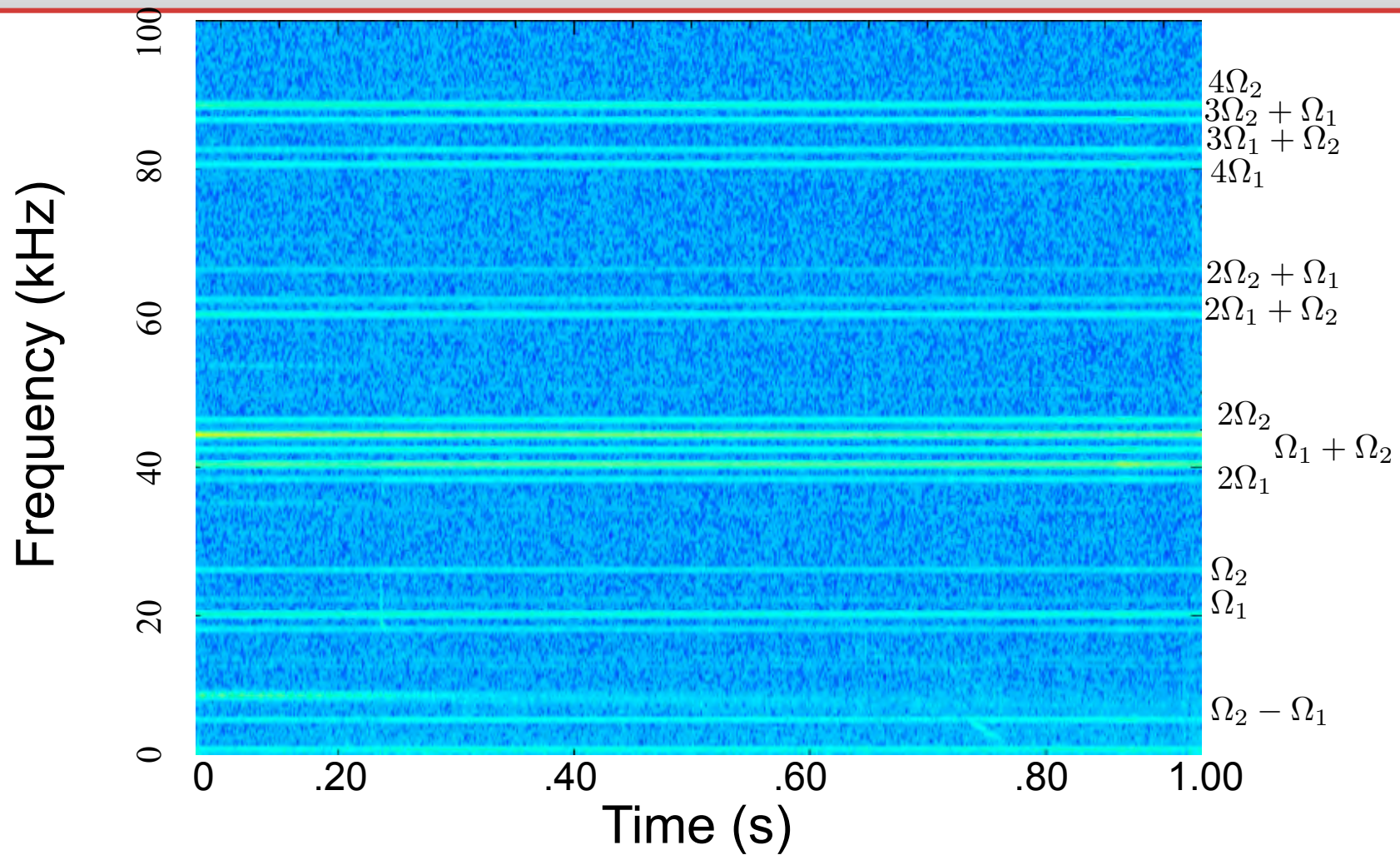
- Polarimeter equation with fluctuating density ( $\alpha \sin(\omega t)$ ) and magnetic ( $\tilde{\gamma} \sin(\omega t)$ ) perturbation.
- Polarimeter has two photoelastic modulators (PEM's) modulated at  $\Omega_1$  and  $\Omega_2$ .

## Fluctuations Observed in MSE Data

$$\begin{aligned}
 I = & I_0 \left( 1 + \frac{J_0(\pi)}{\sqrt{2}} \{ \cos(2\gamma) + \sin 2(\gamma) \} \right. \\
 & \left. + \sin(\omega t) \left( \alpha \frac{J_0(\pi)}{\sqrt{2}} \{ \sin(2\gamma) + \cos(2\gamma) \} + \alpha + \sqrt{2} J_0(\pi) \tilde{\gamma} \{ \cos(2\gamma) - \sin(2\gamma) \} \right) \right. \\
 & - \cos(2\Omega_1 t) \sqrt{2} J_2(\pi) \cos(2\gamma) \\
 & - \cos(2\Omega_2 t) \sqrt{2} J_2(\pi) \sin(2\gamma) \\
 & + \{ \sin((2\Omega_1 - \omega)t) - \sin((2\Omega_1 + \omega)t) \} \left[ \frac{J_2(\pi)}{\sqrt{2}} \left\{ 2\tilde{\gamma} \sin(2\gamma) - \alpha \cos(2\gamma) \right\} \right] \\
 & - \{ \sin((2\Omega_2 - \omega)t) - \sin((2\Omega_2 + \omega)t) \} \left[ \frac{J_2(\pi)}{\sqrt{2}} \left\{ 2\tilde{\gamma} \cos(2\gamma) + \alpha \sin(2\gamma) \right\} \right] \\
 & + \dots
 \end{aligned}$$

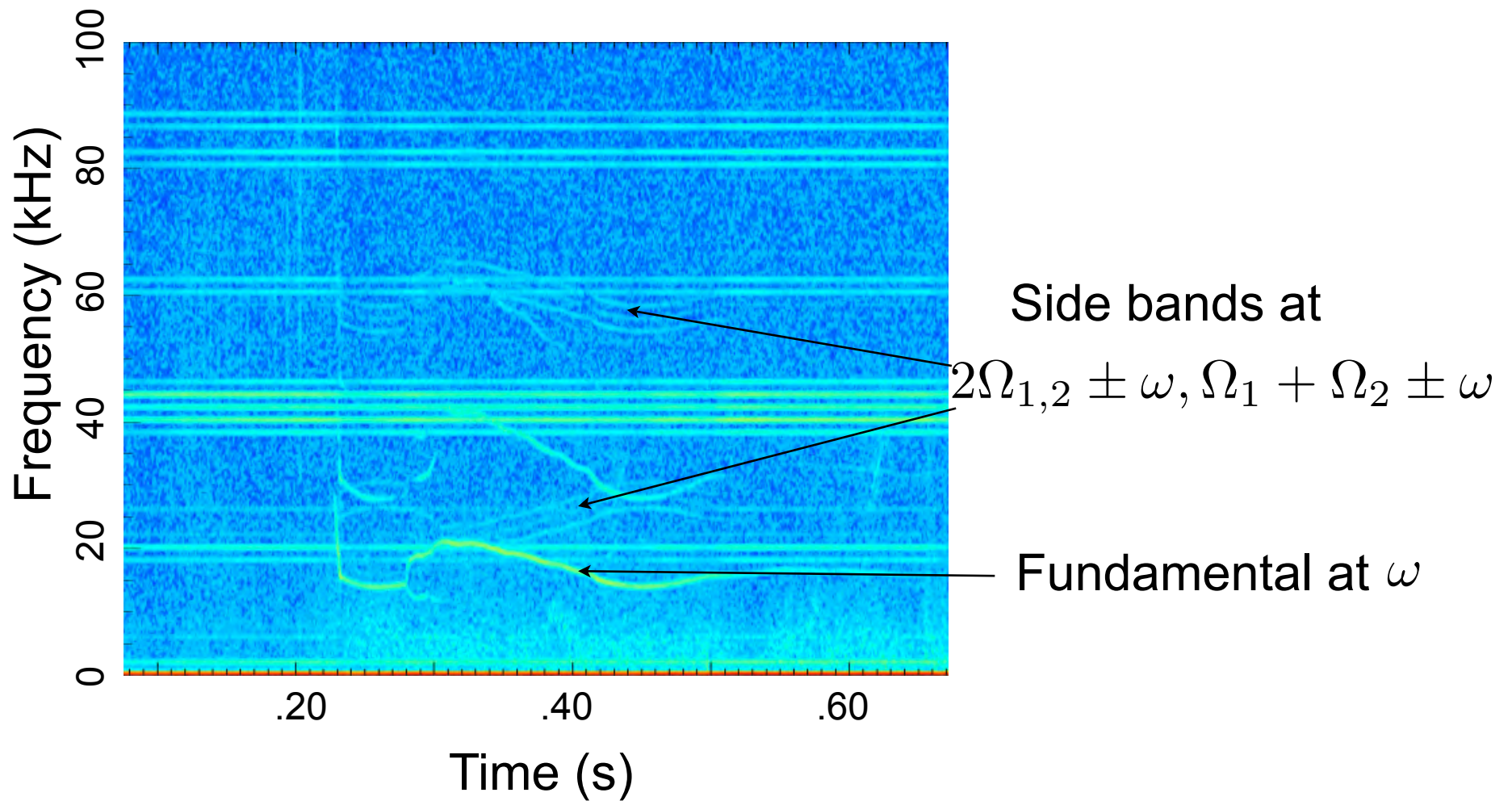
- Expansion of polarimeter equation shows sideband frequency distribution of fluctuations.

## MSE Power Spectra



- No apparent fluctuations besides polarimeter frequencies (20 and 22 kHz) from photoelastic modulators.

## MSE Spectra with Fluctuations



## Summary

- The MSE-CIF diagnostic on NSTX presently has 16 channels operational with 19 available for future upgrades. Novel tunable birefringent interference filter design working well. Makes MSE measurements possible at low magnetic field.
- Upgrade to improve filter transmission by a factor of three is underway.
- Routinely used for physics analysis with LRDFIT equilibrium reconstruction code.
- MHD can have a strong effect on the current profile evolution.
- Sawtooth reconnection is observed to raise  $q(0)$ .
- Coherent magnetic/density fluctuations have been observed with high throughput MSE system.